CHEMISTRY
A EUROPEAN JOURNAL

DOI: 10.1002/chem.200800070

Regulation of the Near-IR Spectral Properties of Individually Dissolved Single-Walled Carbon Nanotubes in Aqueous Solutions of dsDNA

Yuichi Noguchi, Tsuyohiko Fujigaya, Yasuro Niidome, and Naotoshi Nakashima*[a]

Abstract: Two different single-walled carbon nanotubes (SWNTs), the so-called HiPco and CoMoCAT, have been individually dissolved in aqueous solutions of double-stranded DNA (dsDNA). Atomic force microscopy (AFM) revealed the fine structures of the dsDNA-wrapped SWNTs. The near-IR absorption and photoluminescence (PL) spectra of aqueous solutions of dsDNA-wrapped SWNTs were recorded and, in pure water, we observed only a single two-dimensional PL spot from (6,5) SWNTs for both HiPco and CoMoCAT. In sharp contrast, when Tris-EDTA (TE) buffer was used in place of pure water, the PL-mapping images of the solutions showed chirality indices of (6,5), (7,5), (7,6), (8,4), (9,4), and (10,2) for HiPco-SWNTs, and (6,5) and (7,5) for CoMoCAT-SWNTs. The first semiconducting bands in the near-IR absorption spectra of solutions of dsDNA-wrapped SWNTs are different. To explain the observed differences in the near-IR absorption and PL behavior we conducted several experiments and found that the near-IR optical properties of the SWNTs can be modulated by changing the pH of the solutions. The pH breakpoints for near-IR absorption bleaching and PL quenching are different and the phenomena are explained by differences in the numbers of holes generated on the SWNTs. These findings are important from both fundamental and applied viewpoints.

Keywords: DNA · nanotubes · NIR spectroscopy · pH effects · photoluminescence

Introduction

Since their discovery in 1991,[1] carbon nanotubes (CNTs) have been at the forefront of nanoscience and nanotechnology because of their remarkable electrical, mechanical, thermal, and optical properties.[2–8] Their potential applications are, however, often limited because of their insolubility in many solvents due to strong internanotube van der Waals forces. Therefore, strategic approaches to the solubilization of CNTs are important for realizing the potential applications of CNTs.[9–13] The combination of CNTs and DNA (or RNA) is of great interest in many chemical and biochemical areas. We have already reported the finding that single-walled carbon nanotubes (SWNTs) dissolve in aqueous solutions of double-stranded DNA (dsDNA).[14] The method is quite simple: SWNTs are placed in an aqueous solution of dsDNA and then sonicated with a bath-type sonicator at temperatures below 10 °C to produce SWNT/dsDNA solutions/dispersions that are stable for more than six months upon storage at 5 °C.[14] We later showed that electrochemical deposition of SWNT–dsDNA complexes by poly(ethylenedioxythiophene) (poly(EDOT)) on an indium tin oxide (ITO) electrode is possible.[15]

A number of groups have now used this procedure in their studies of various dsDNA and CNT structures. Barisci et al.[16] fabricated SWNT/dsDNA fibers that were mechanically strong and conductive, and that exhibited useful capacitance values of up to 7.2 $F g^{-1}$. Iijima et al.[17] produced high-resolution TEM and STM images of dsDNA/multi-walled CNTs. Gladchenko et al.[18] characterized fragmented dsDNA-wrapped SWNTs in aqueous solutions. He and Bayachou[19] described the layer-by-layer fabrication and characterization of dsDNA-wrapped SWNT particles. Prato and co-workers[20] described the binding of plasmid DNA onto functionalized CNTs in the construction of CNT-based gene-transfer vector systems. Dordick and co-workers[21] reported in vitro transcription and protein translation from CNT/DNA assemblies. Coleman and co-workers[22] reported the spontaneous dispersion of SWNTs by dsDNA.

At the same time as we published our report on the solubilization of SWNTs by dsDNA, Zheng and co-workers[23,24]

[a] Y. Noguchi, Dr. T. Fujigaya, Prof. Y. Niidome, Prof. N. Nakashima
Department of Applied Chemistry, Graduate School of Engineering
Kyushu University, 744 Motooka, Fukuoka 819-0395 (Japan)
Fax: (+81) 92-802-2840
E-mail: nakashima-tcm@mail.cstm.kyushu-u.ac.jp

showed that single-stranded DNA (ssDNA) also solubilizes SWNTs. Many papers describing the properties of SWNT/ssDNA composites have since been published. One interesting finding was the ability to separate metallic and semi-conducting SWNTs by using size-exclusion chromatography.[25] Molecular modeling of SWNT/ssDNA composites suggests that ssDNA can bind to SWNTs through π-stacking, which results in the helical wrapping of SWNTs.[23] Zhao and Johnson[26] reported a molecular dynamics simulation of DNA adsorption on a SWNT in an aqueous environment. A binding model for a (10,0) SWNT wrapped in poly(T) has been reported and the binding of ssDNA to SWNTs has been probed by flow linear dichroism.[27,28] Detailed optical properties, including near-IR absorption and photoluminescence (PL) properties, and a Raman study of CoMoCAT-SWNT/ssDNA hybrids have been reported.[29,30] Very recently, Fagan et al.[31] described length-dependent optical effects in SWNTs dissolved in ssDNA (30-mer). SWNT/ssDNA solutions have been used to explore the solution redox chemistry of CNTs,[32] photoinduced charge transfer to an Ag^+/DNA/CNT complex,[33] and electrocatalytic oxidation.[34] Phonon-assisted excitation dynamics for (6,5)-enriched ssDNA-wrapped SWNTs have been discussed theoretically.[35,36] The adsorption behavior of ssDNA-wrapped SWNTs on substrates has been examined by reflection absorption FTIR and Raman spectroscopy and by XPS.[37] Recently, Strano and co-workers[38] reported that the optical detection of DNA conformational polymorphism on SWNTs is possible. Li et al.[39] showed that CNTs selectively destabilize duplex and triplex DNA and induced a B–A transition in solution. DNA-immobilized aligned carbon nanotubes have been shown to be important for sensing complementary DNA and/or target DNA chains of specific sequences with a high sensitivity and selectivity.[40] Fantini et al.[41] characterized GT-DNA oligomer-wrapped SWNTs by Raman and optical spectroscopy and revealed different interactions for semi-conducting and metallic SWNTs. Chou et al.[42] described in detail the length characterization of ssDNA-wrapped SWNTs by using Raman spectroscopy. Recently, racemic SWNTs were found to exhibit circular dichroism when wrapped with ssDNA oligomer $d(GT)_{20}$.[43] Golovchenko and co-workers[44] measured the optical absorbance spectra of SWNTs dispersed by ssDNA homopolymers and found that the anisotropic absorbance of SWNTs leads to a large anisotropic hypochromicity in the attacked DNA bases. We have constructed multilayer assemblies with alternating monolayers of poly(G)- and poly(C)-wrapped SWNTs on quartz based on the complementary base-pairing between nucleic bases G and C, which have applications in a wide range of fields of nanoscience and technology.[45] SWNT/ssDNA (RNA) solutions can be used as materials for gene and protein delivery and nanotherapy.[46] Onoa et al.[47] reported that DNA(RNA)/CNT hybrids are playing an important role in the rapid development of nanotechnologies. Douglas et al. reported SWNT/ssDNA-induced alignment of membrane proteins for NMR structure determination.[48] Deng and co-workers[49] reported that ssDNA-wrapped SWNTs can serve well as rigid templates for the self-assembly of gold nanoparticles. Mao and co-workers[50] fabricated nanohybrids of ssDNA-wrapped SWNTs and DNA-modified gold nanoparticles by using DNA hybridization methods.

Herein we describe the regulation of the near-IR optical properties of individually dissolved SWNTs in aqueous solutions of dsDNA. Near-IR PL mapping of individually solubilized SWNTs in pure water showed only one spot from the (6,5) SWNTs, and their PL behavior dramatically changed with pH. A possible mechanism for the tunable near-IR optical behavior is presented. The fine structures of dsDNA-wrapped SWNTs revealed by atomic force microscopy are also described.

Results and Discussion

Fine structures of SWNT/dsDNA: We have already reported an AFM image of an aqueous solution of SWNT/dsDNA[14] and Zhao and co-workers[51] have reported an AFM image of dsDNA-wrapped SWNTs. Here we show the fine structures of an aqueous solution of SWNT/dsDNA, which were obtained by atomic force microscopy (AFM). Typical images are shown in Figure 1. The magnified images shown in Figure 1B, C strongly suggest that the SWNTs are wrapped by the DNA. As shown in Figure 1C, the heights of the tubes were found to range from 1.4 to 2.4 nm, which indicates the existence of individually dissolved SWNTs in so-

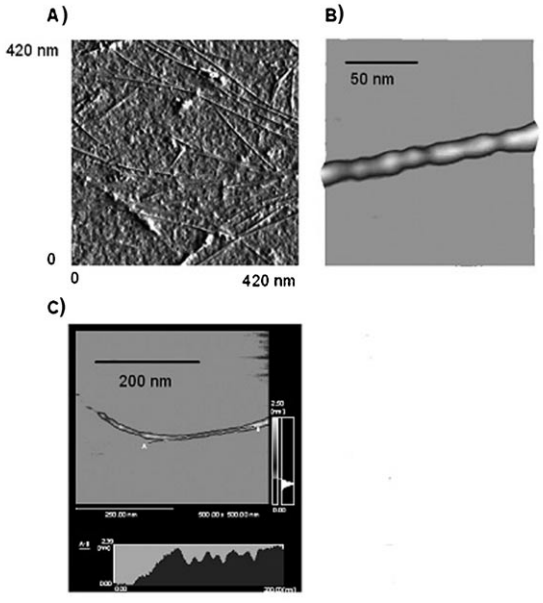

Figure 1. Typical AFM images on mica of the SWNTs dissolved in an aqueous solution of dsDNA. Figure 1C shows the height profile of the AFM image of the solution together with the AFM image. The Images A, B, and C were produced with a Veeco, a NanoScope IIIa (phase mode), and a Shimadzu Nanosearch Microscope SFT-3500 (dynamic mode), respectively (for details, see the Experimental Section).

lution because the diameter of the SWNTs used is ≈0.7–1 nm and the thickness of the dsDNA is 1.5 nm. A schematic illustration of the DNA-wrapped SWNTs is shown in Figure 2. The weak interaction between the major (and/or minor) grooves of the DNA and the nanotubes might contribute to the dissolution.

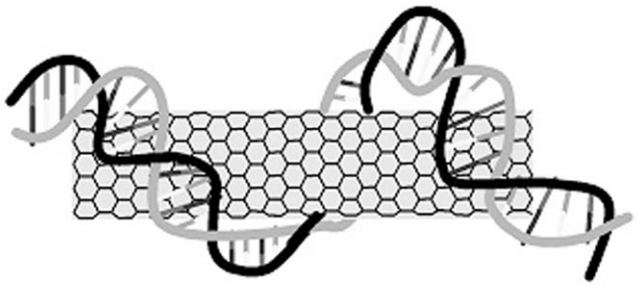

Figure 2. Schematic drawing of a dsDNA-wrapped SWNT.

Modulation of the near-IR optical properties of SWNTs in solutions of dsDNA

Spectral properties of HiPco-SWNTs in Milli-Q water: The characteristic absorption bands in the near-IR region due to the interband transition between the mirror image spikes in the density of states (DOS) of the SWNTs are a powerful way to characterize the optical properties of SWNTs. Weisman and co-workers[52] reported that raw SWNTs dissolved in an aqueous micelle of sodium dodecyl sulfate (SDS) individually showed photoluminescence (PL) in the near-IR region. Since their report, considerable attention has been focused on this unique optical behavior.[53] Figure 3A (dotted line) and B show the near-IR absorption and 2D-PL mapping (2D excitation/emission contour map) image of HiPco-SWNTs dissolved in pure water, respectively. We see characteristic absorption spectral features in the near-IR region that indicate the existence of metallic and semiconducting SWNTs. Note that the PL-mapping image revealed that only SWNTs with the chirality index (6,5) strongly fluoresce. The data imply the following three possibilities, that is, that the DNA in Milli-Q water 1) individually solubilizes only (6,5) SWNTs, 2) individually solubilizes only (6,5) SWNTs whereas the SWNTs with other chirality indices are dispersed as bundled structures, or 3) individually solubilizes the SWNTs with many chirality indices, but the PL from SWNTs with chiral indices other than (6,5) is quenched. To reveal which is the real situation, we added an aqueous solution of sodium hydroxide to the SWNT/dsDNA solution; the result is shown in Figure 3A (solid line) and C and suggests that the third possibility is the real one. To characterize the mechanism of the NIR absorption bleaching and PL quenching of the SWNT/dsDNA solutions in detail, we conducted experiments in buffer solutions.

Optical properties of HiPco-SWNTs in buffer solutions: Tris-EDTA TE buffer solutions are widely used in dsDNA studies. In Figure 4A (solid line) and B, we show, respectively, the NIR absorption spectra and 2D-PL-mapping image for HiPco-SWNTs in a TE buffer solution (pH 8.0). The results are quite different to those obtained in pure water (shown in Figure 4A, dotted line for comparison). In the TE buffer solution we see well-resolved near-IR bands in the range 1000–1200 nm, which arise from the first semi-conducting band of the SWNTs, and the existence of SWNTs with chirality indices of (6,5), (7,5), (7,6), (8,4), (9,4), and (10,2).

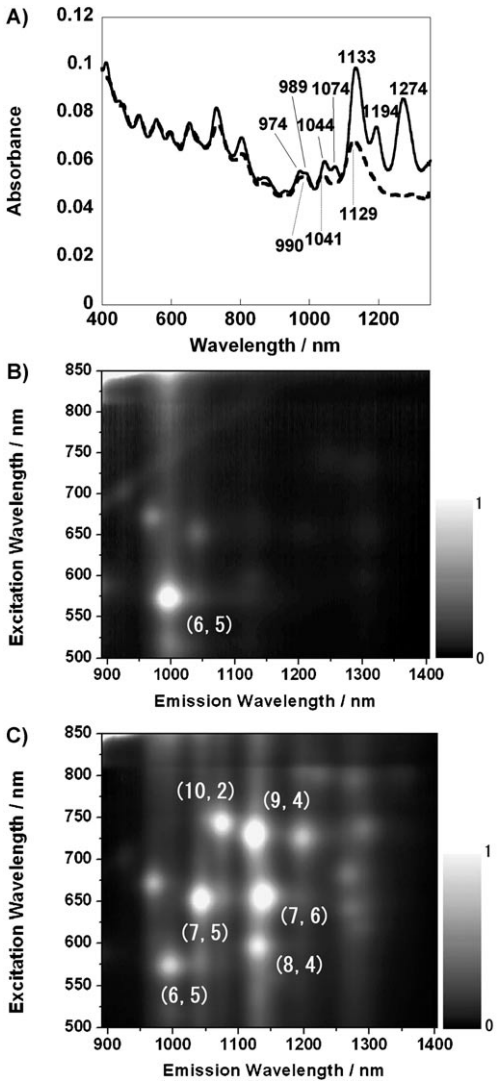

Figure 3. A) Vis/NIR absorption spectra (dotted line: pure water; solid line: alkaline solution at pH 8.7) and PL mapping images of HiPco-SWNTs dissolved in a solution of dsDNA in B) pure water and C) an alkaline solution.

Optical properties of CoMoCAT-SWNTs: A similar experiment using CoMoCAT-SWNTs in place of HiPco-SWNTs was carried out and the results obtained are shown in Figure 5. In pure water, the peak seen at 1272 nm in the buffer was bleached and those at around 1127, 1035, and 984 nm decreased. In pure water, again the PL mapping shows fluorescence only from CoMoCAT-SWNTs with the

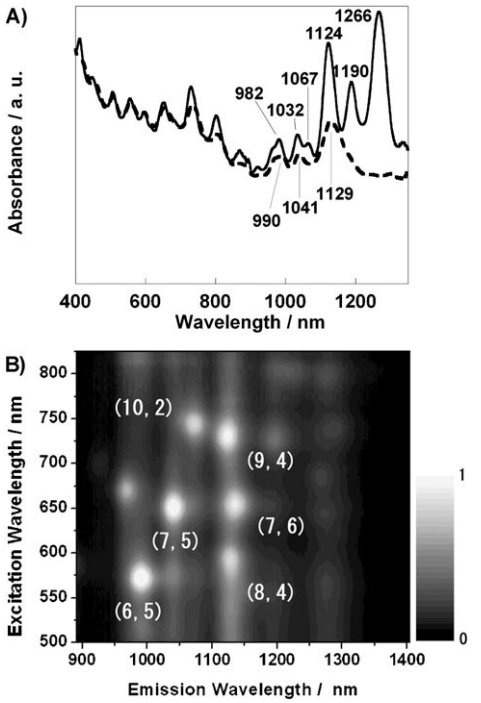

Figure 4. A) Vis/NIR absorption spectra (dotted line: pure water; solid line: TE buffer at pH 8.0) and B) PL-mapping image of HiPco-SWNTs dissolved in a solution of dsDNA in TE buffer.

chirality index (6,5) (Figure 5B), whereas in TE buffer, we see both (6,5) and (7,5) chirality indices in the PL-mapping image (Figure 5C). Because CoMoCAT-SWNTs are rich in the (6,5) and (7,5) chirality indices, the result is understandable.

pH dependence: Figures 6 and 7 show the near-IR absorption spectra and the PL-mapping images of HiPco-SWNT/DNA in phosphate buffers at specific pH values. The near-IR absorption spectrum at pH 5.8 shows peaks at 984, 1031, and 1120 nm in the first semiconducting bands, which changed drastically at pH 6.4, that is, peaks appeared at 984, 1043, 1132, 1193, and 1268 nm. The spectra obtained at pHs 7.0 and 8.0 are similar to that at pH 6.4, that is, the near-IR absorption spectral change occurred at around pH 6. The PL-mapping images also show a strong pH dependence. As can be seen in Figure 7, we only see one spot at pH 5.8, which is from the (6,5) SWNTs, and at pH 6.4 we observed the spot from the (6,5) SWNTs together with a weak emission spot from the (8,4) SWNTs. A drastic change in the PL-mapping image occurred at pH 7.0, with emission spots from SWNTs with chirality indices of (6,5), (7,5), (7,6), (8,4), (9,4), and (10,2). Similar behavior was observed at pH 8.0. Note that the pH at which the near-IR absorption spectra and PL-mapping images change are different. Zhao and co-workers[54] briefly described the pH response of the near-IR absorption spectra of HiPco-SWNTs dissolved in an aqueous solution of dsDNA (salmon testes). However, they did not describe the PL data of the solutions. Their near-IR

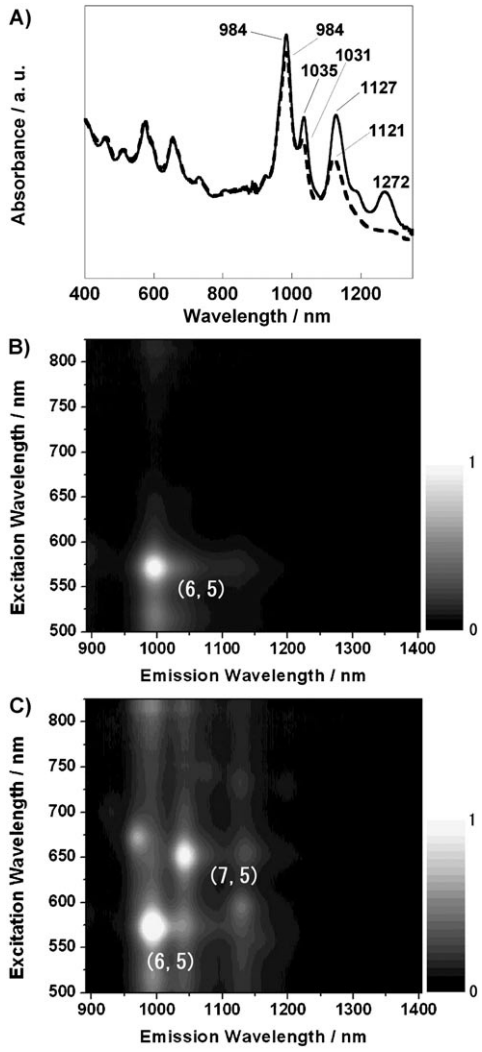

Figure 5. A) Vis/NIR absorption spectra (dotted line: pure water; solid line: TE buffer at pH 8.0) and PL-mapping images of CoMoCAT-SWNTs dissolved in solutions of dsDNA in B) pure water and C) TE buffer.

absorption spectra resemble ours, but the S11 band structures are much sharper in ours and the pH dependence is somewhat different. Very recently, Wang and Chen[55] reported the pH response of the near-IR absorption spectra of an aqueous solution of poly(L-lysine)/SWNTs, whereas the pH dependence of the PL spectra was not as drastic as with our SWNT/dsDNA system.

The pH dependence of the CoMoCAT-SWNTs was similarly examined and the results are shown in Figure 8 and Figure 9. It was found that the pH-dependent near-IR optical properties of CoMoCAT-SWNTs in an aqueous solution of dsDNA resemble those of HiPco-SWNTs, namely, the NIR absorption spectra change between pH 5.8 and 6.4. The change in the PL is more distinct between pH 6.4 and 7.0.

Mechanism of absorption bleaching and PL quenching: The observed pH dependence can be explained as follows. Strano et al.[56] reported pH-dependent near-IR absorption

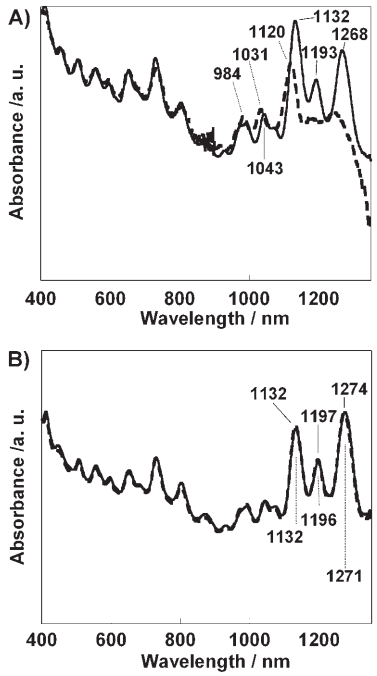

Figure 6. Vis/NIR absorption spectra of HiPco-SWNTs dissolved in phosphate buffer solutions of dsDNA at A) pH 5.8 (dotted line), 6.4 (solid line), B) 7.0 (dotted line), and 8.0 (solid line).

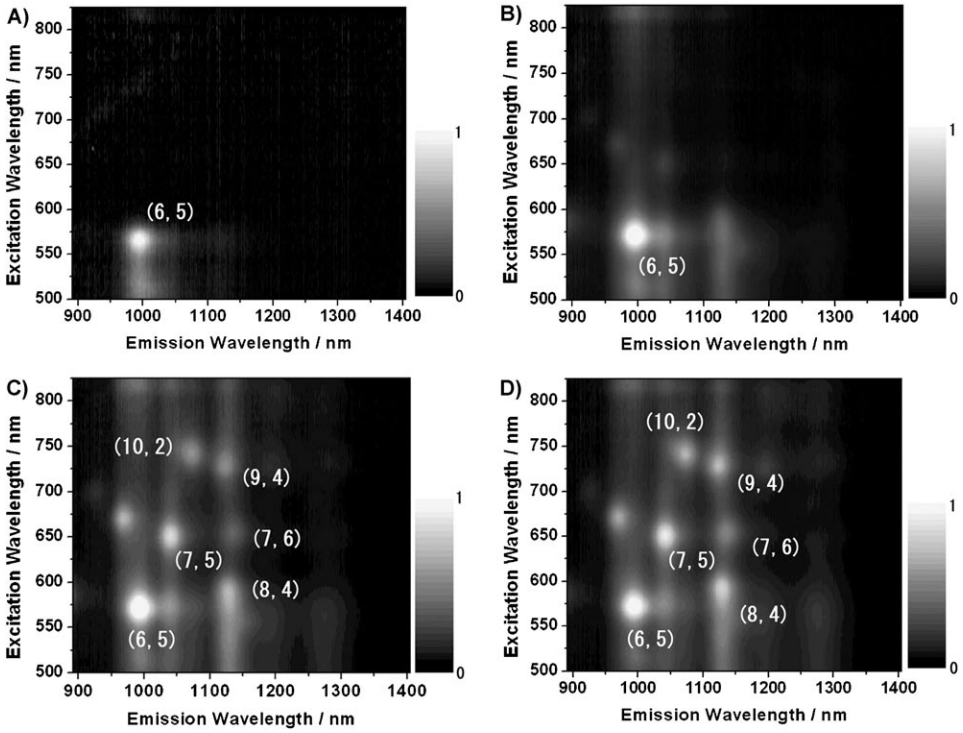

Figure 7. PL-mapping images of HiPco-SWNTs dissolved in dsDNA in phosphate buffer at pH 5.8, 6.4, 7.0, and 8.0.

spectra for SWNTs dissolved in an aqueous micelle of SDS in which all S11 semi-conducting peaks in the range 1000–1600 nm almost disappeared at pHs below pH 5.0. The observed pH dependence was explained by the protonation of the SWNTs, which induces a change in the band gap of the nanotubes. Brus and co-workers[57] reported similar pH-dependent near-IR optical behavior for SWNTs dissolved in an aqueous micellar solution of poly(maleic acid/octyl vinyl ether). They explained the behavior in terms of reversible SWNT oxidation by analyzing the oxide-induced absorption bleaching and luminescence quenching at low pHs. In this study, the absorption bleaching and luminescence quenching phenomena observed for solutions of SWNT/dsDNA can fundamentally be explained by a similar mechanism. An interesting feature of this study is that in the SWNT/dsDNA solutions we only see a single PL spot from the (6,5) SWNTs, which are almost the smallest-diameter SWNTs (diameter = 0.757 nm) for both HiPco and CoMoCAT at the low pHs. How, then, do we explain the observed distinct size-selective PL behavior?

Recently, Doorn and co-workers[58] described the chiral selectivity of metallic and semi-conducting SWNTs in the charge-transfer bleaching of the near-IR spectra of individually dissolved SWNTs in a SDS micelle in the presence of an organic acceptor molecule. In this study, however, we did not add such a redox compound. Note that in this work, the SWNT/dsDNA solutions show size-selective PL behavior in pure water and in buffers at low pHs. Another interesting feature is that the pH break-point for PL quenching is shifted relative to that of the near-IR absorption bleaching, that is, at pH 6.4 we see only one PL spot from the (6,5) SWNTs (see Figure 7), whereas the near-IR absorption has already recovered at this pH. For 400-nm-length SWNTs, more than 250 holes are reported to be necessary for absorption bleaching, whereas around 10 holes are sufficient for PL quenching.[57] Based on the PL quenching mechanisms of Strano,[56] Brus,[57] and Doorn[58] and their co-workers, the phenomena can be explained by the protonation of the SWNTs followed by the generation of holes on the surfaces of the SWNTs. This explains the difference in the pH dependence of the NIR absorption spectra and PL mapping of aqueous solutions of SWNT/dsDNA, that is, as we described in the section on pH dependence, the pH break-point of the PL appears at a higher pH, at which the concentration of the proton is smaller, than that of the NIR absorption spectra. The proposed mechanism is also applicable to CoMo-

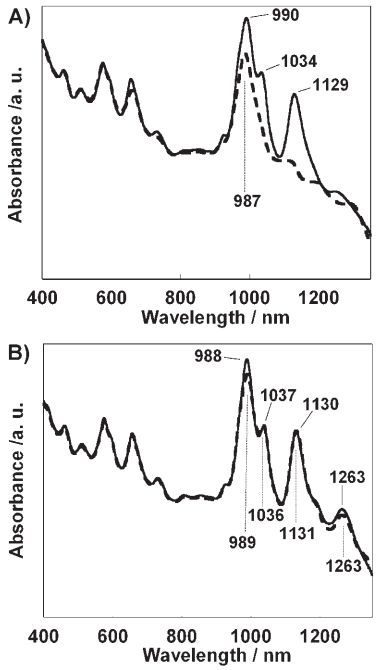

Figure 8. Vis/NIR absorption spectra of CoMoCAT-SWNTs dissolved in phosphate buffer solutions of dsDNA at A) pH 5.8 (dotted line), 6.4 (solid line), B) 7.0 (dotted line), and 8.0 (solid line).

CAT-SWNTs because both forms of SWNTs showed a similar pH dependence.

Conclusion

In this report we have described the well-resolved structure of dsDNA-wrapped SWNTs and then shown that the modulation of the band gaps of individually solubilized SWNTs (HiPco and CoMoCAT) in aqueous solutions of dsDNA is possible by changing the pH of the solutions. We would like to emphasize that a very small pH change (from pH 5.8 to 6.4 in near-IR absorption spectroscopy, and from pH 6.4 to 7.4 in PL) causes a dramatic spectral change. We have explained the results in terms of reversible SWNT oxidation by analysis of oxide-induced absorption bleaching and luminescence quenching at low pHs, and the difference in the observed pH break-points for the near-IR absorption bleaching and PL quenching are due to the difference in the numbers of holes generated on the SWNTs. The results obtained in this study are fundamentally important and useful for understanding the optical band gap properties of individually dissolved SWNTs in aqueous solutions of dsDNA. Also, this finding might afford the opportunity to design and develop a novel device based on SWNT/dsDNA nano-biomaterials.

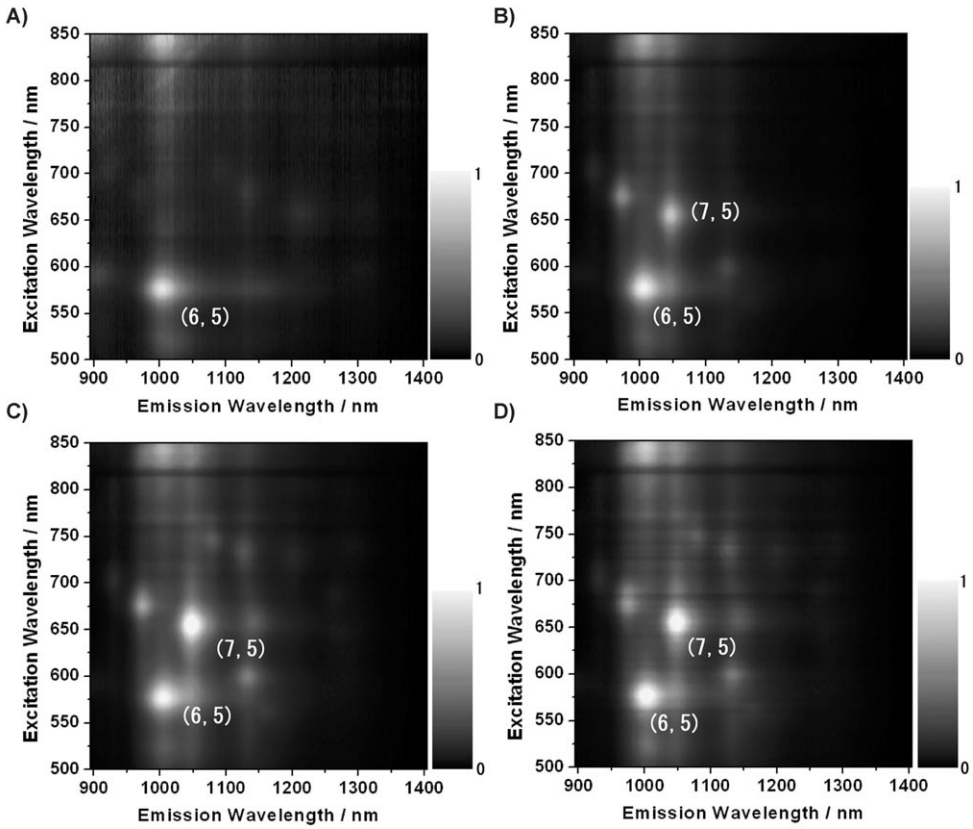

Figure 9. PL-mapping images of CoMoCAT-SWNTs dissolved in phosphate buffer solutions of dsDNA at pH 5.8, 6.4, 7.0, and 8.0.

Experimental Section

DNA (salmon testes, 300 bp, lot No. 040217) was kindly provided by Nichiro Corporation and used as received. SWNTs were purchased from Carbon Nanotechnology Inc. (HiPco) and South West Nanotechnologies (CoMoCAT) and used as received. Aqueous solutions of SWNT/DNA were prepared similarly to a procedure described elsewhere.[14] Typically, SWNTs (0.5 mg) were added to DNA (0.68 mg mL^{-1}) dissolved in pure water (5.0 mL) or buffer (5.0 mL) and sonicated with a bath-type ultrasonic cleaner (Branson 2210) at temperatures below 5 °C for 1 h, followed by centrifugation at 250000*g* for 4 h (Hitachi himac CS 100GXL). The UV/visible/NIR and photoluminescence spectra of aqueous solutions of SWNT/DNA were recorded at 25±1 °C on a V-570 JASCO and a HORIBA JOBIN YVON spectrophotometer (Fluorolog^{R}-3 with FluorEssence), respectively. A freshly cleaved mica substrate was dipped into an aqueous solution for a few seconds, dried in a vacuum, and atomic force microscope (AFM) images of the samples thus obtained were recorded on a Veeco, NanoScope IIIa, or Shimadzu Nanosearch Microscope SFT-3500 instrument.

Acknowledgements

This work was supported by Grants-in-Aid for Exploratory (No. 18651059) and Scientific Research (A) (No. 17205014) and the Promotion of Novel Interdisciplinary Fields Based on Nanotechnology and Materials from the Ministry of Education, Culture, Sports, Science and Technology, Japan.

[1] S. Iijima, *Nature* **1991**, *354*, 56–58.
[2] P. J. F. Harris, *Carbon nanotubes and related structures: New materials for the 21st Century*, Cambridge University Press, New York, **1999**.
[3] S. Reich, C. Thomsen, J. Maultzsch, *Carbon Nanotubes: Basic Concepts and Physical Properties*, Wiley-VCH, Weinheim, **2004**.
[4] M. Meyyappan, *Carbon Nanotubes: Science and Applications*, CRC Press, New York, **2005**.
[5] S. V. Rotkin, S. Subramoney, *Applied Physics of Carbon Nanotubes: Fundamentals of Theory, Optics and Transport Devices*, Springer, New York, **2005**.
[6] *Understanding Carbon Nanotubes* (Ed.: A. Loiseau, P. Launois, P. Petit, S. Roche, J. P. Salvetat) *[In: Lect. Notes Phys.* **2006**, 677.
[7] *Carbon Nanotubes: Properties and Applications* (Ed.: M. J. O'Connell), CRC Press, New York, **2006**.
[8] G. Dresselhaus, M. S. Dresselhaus, P. Avouris, *Carbon Nanotubes: Synthesis, Structure, Properties and Applications*, Springer, Berlin, **2001**.
[9] N. Nakashima, *Int. J. Nanosci.* **2005**, *4*, 119–137.
[10] H. Murakami, N. Nakashima, *J. Nanosci. Nanotechnol.* **2006**, *6*, 16–27.
[11] D. Tasis, N. Tagmatarchis, A. Bianco, M. Prato, *Chem. Rev.* **2006**, *106*, 1105–1136.
[12] N. Nakashima, T. Fujigaya, *Chem. Lett.* **2007**, *36*, 692–697.
[13] A. Hirsch, *Angew. Chem.* **2002**, *114*, 1933–1939; *Angew. Chem. Int. Ed.* **2002**, *41*, 1853–1859.
[14] N. Nakashima, S. Okuzono, H. Murakami, T. Nakai, K. Yoshikawa, *Chem. Lett.* **2003**, *32*, 456–457.
[15] A.-H. Bae, T. Hatano, N. Nakashima, H. Murakami, S. Shinkai, *Org. Biomol. Chem.* **2004**, *2*, 1139–1144.
[16] J. N. Barisci, M. Tahhan, G. G. Wallace, S. Badaire, T. Vaugien, M. Maugey, P. Poulin, *Adv. Funct. Mater.* **2004**, *14*, 133–138.
[17] M. Iijima, T. Watabe, S. Ishii, A. Koshio, T. Yamaguchi, S. Bandow, S. Iijima, K. Suzuki, Y. Maruyama, *Chem. Phys. Lett.* **2005**, *414*, 520–524.
[18] G. O. Gladchenko, M. V. Karachevtsev, V. S. Leontiev, V. A. Valeev, A. Y. Glamazda, A. M. Plokhotnichenko, S. G. Stepanian, *Mol. Phys.* **2006**, *104*, 3193–3201.
[19] P. He, M. Bayachou, *Langmuir* **2005**, *21*, 6086–6092.
[20] D. Pantarotto, R. Singh, D. McCarthy, M. Erhardt, J.-P. Briand, M. Prato, K. Kostarelos, A. Bianco, *Angew. Chem.* **2004**, *116*, 5354–5358; *Angew. Chem. Int. Ed.* **2004**, *43*, 5242–5246.
[21] K. Rege, G. Viswanathan, G. Zhu, A. Vijayaraghavan, P. M. Ajayan, J. S. Dordick, *Small* **2006**, *2*, 718–722.
[22] H. Cathcart, S. Quinn, V. Nicolosi, J. M. Kelly, W. J. Blau, J. N. Coleman, *J. Phys. Chem. C* **2007**, *111*, 66–74.
[23] M. Zheng, A. Jagota, E. D. Semke, B. A. Diner, R. S. McLean, S. R. Lustig, R. E. Richardson, N. G. Tassi, *Nat. Mater.* **2003**, *2*, 338–342.
[24] M. Zheng, A. Jagota, M. S. Strano, A. P. Santos, P. Barone, S. G. Chou, B. A. Diner, M. S. Dresselhaus, R. S. McLean, G. B. Onoa, G. G. Samsonidze, E. D. Semke, M. Usrey, D. J. Walls, *Science* **2003**, *302*, 1545–1548.
[25] X. Huang, R. S. McLean, M. Zheng, *Anal. Chem.* **2005**, *77*, 6225–6228.
[26] X. Zhao, J. K. Johnson, *J. Am. Chem. Soc.* **2007**, *129*, 10438–10445.
[27] J. Rajendra, M. Baxendale, L. G. D. Rap, A. Rodger, *J. Am. Chem. Soc.* **2004**, *126*, 11182–11188.
[28] J. Rajendra, A. Rodger, *Chem. Eur. J.* **2005**, *11*, 4841–4847.
[29] S. G. Chou, H. B. Ribeiro, E. B. Barros, A. P. Santos, D. Nezich, G. G. Samsonidze, C. Fantini, M. A. Pimenta, A. Jorio, F. Plentz Filho, M. S. Dresselhaus, G. Dresselhaus, R. Saito, M. Zheng, G. B. Onoa, E. D. Semke, A. K. Swan, M. S. Uenlue, B. B. Goldberg, *Chem. Phys. Lett.* **2004**, *397*, 296–301.
[30] H. Kawamoto, T. Uchida, K. Kojima, M. Tachibana, *J. Appl. Phys.* **2006**, *99*, 094309/1–094309/4.
[31] J. A. Fagan, J. R. Simpson, B. J. Bauer, S. H. Lacerda, M. L. Becker, J. Chun, K. Migler, A. R. H. Walker, E. K. Hobbie, *J. Am. Chem. Soc.* **2007**, *129*, 10607–10612.
[32] M. Zheng, B. A. Diner, *J. Am. Chem. Soc.* **2004**, *126*, 15490–15494.
[33] M. Zheng, V. V. Rostovtsev, *J. Am. Chem. Soc.* **2006**, *128*, 7702–7703.
[34] M. E. Napier, D. O. Hull, H. H. Thorp, *J. Am. Chem. Soc.* **2005**, *127*, 11952–11953.
[35] S. G. Chou, M. F. DeCamp, J. Jiang, G. G. Samsonidze, E. B. Barros, F. Plentz, A. Jorio, M. Zheng, G. B. Onoa, E. D. Semke, A. Tokmakoff, R. Saito, G. Dresselhaus, M. S. Dresselhaus, *Phys. Rev. B* **2005**, *72*, 195415/1–195415/8.
[36] S. G. Chou, F. Plentz, J. Jiang, R. Saito, D. Nezich, H. B. Ribeiro, A. Jorio, M. A. Pimenta, G. G. Samsonidze, A. P. Santos, M. Zheng, G. B. Onoa, E. D. Semke, G. Dresselhaus, M. S. Dresselhaus, *Phys. Rev. Lett.* **2005**, *94*, 127402/1–127402/4.
[37] R. A. Zangmeister, J. E. Maslar, A. Opdahl, M. J. Tarlov, *Langmuir* **2007**, *23*, 6252–6256.
[38] D. A. Heller, E. S. Jeng, T.-K. Yeung, B. M. Martinez, A. E. Moll, J. B. Gastala, M. S. Strano, *Science* **2006**, *311*, 508–511.
[39] X. Li, Y. Peng, X. Qu, *Nucleic Acids Res.* **2006**, *34*, 3670–3676.
[40] P. He, S. Li, L. Dai, *Synth. Met.* **2005**, *154*, 17–20.
[41] C. Fantini, A. Jorio, A. P. Santos, V. S. T. Peressinotto, M. A. Pimenta, *Chem. Phys. Lett.* **2007**, *439*, 138–142.
[42] S. G. Chou, H. Son, J. Kong, A. Jorio, R. Saito, M. Zheng, G. Dresselhaus, M. S. Dresselhaus, *Appl. Phys. Lett.* **2007**, *90*, 131109/1–131109/3.
[43] G. Dukovic, M. Balaz, P. Doak, N. D. Berova, M. Zheng, R. S. McLean, L. E. Brus, *J. Am. Chem. Soc.* **2006**, *128*, 9004–9005.
[44] M. E. Hughes, E. Brandin, J. A. Golovchenko, *Nano Lett.* **2007**, *7*, 1191–1194.
[45] A. Ishibashi, Y. Yamaguchi, H. Murakami, N. Nakashima, *Chem. Phys. Lett.* **2006**, *419*, 574–577.
[46] N. W. S. Kam, M. O'Connell, J. A. Wisdom, H. Dai, *Proc. Natl. Acad. Sci. USA* **2005**, *102*, 11600–11605.
[47] B. Onoa, M. Zheng, M. S. Dresselhaus, B. A. Diner, *Phys. Status Solidi A* **2006**, *203*, 1124–1131.
[48] S. M. Douglas, J. J. Chou, W. M. Shih, *Proc. Natl. Acad. Sci. USA* **2007**, *104*, 6644–6648.
[49] X. Han, Y. Li, Z. Deng, *Adv. Mater.* **2007**, *19*, 1518–1522.
[50] Y. Chen, H. Liu, T. Ye, J. Kim, C. Mao, *J. Am. Chem. Soc.* **2007**, *129*, 8696–8697.

[51] Y. Xu, P. E. Pehrsson, L. Chen, R. Zhang, W. Zhao, *J. Phys. Chem. C* **2007**, *111*, 8638–8643.
[52] S. M. Bachilo, M. S. Strano, C. Kittrell, R. H. Hauge, R. E. Smalley, R. B. Weisman, *Science* **2002**, *298*, 2361–2366.
[53] R. B. Weisman, *Fluorescence spectroscopy of single-walled carbon nanotubes*, Springer, New York, **2005**.
[54] K. Kelley, P. E. Pehrsson, L. M. Ericson, W. Zhao, *J. Nanosci. Nanotechnol.* **2005**, *5*, 1041–1044.
[55] D. Wang, L. Chen, *Nano Lett.* **2007**, *7*, 1480–1484.
[56] M. S. Strano, C. B. Huffman, V. C. Moore, M. J. O'Connell, E. H. Haroz, J. Hubbard, M. Miller, K. Rialon, C. Kittrell, S. Ramesh, R. H. Hauge, R. E. Smalley, *J. Phys. Chem. B* **2003**, *107*, 6979–6985.
[57] G. Dukovic, B. E. White, Z. Zhou, F. Wang, S. Jockusch, M. L. Steigerwald, T. F. Heinz, R. A. Friesner, N. J. Turro, L. E. Brus, *J. Am. Chem. Soc.* **2004**, *126*, 15269–15276.
[58] M. J. O'Connell, E. E. Eibergen, S. K. Doorn, *Nat. Mater.* **2005**, *4*, 412–418.

Received: January 14, 2008
Published online: May 6, 2008

